[1]J. J. Aubert *et al.*, Phys. Rev. Lett. 33, 1404 (1974).
[2]J.-E. Augustin *et al.*, Phys. Rev. Lett. 33, 1406 (1974); B. Richter, private communications.
[3]M. E. Nordberg, Jr., *et al.*, Rev. Sci. Instrum. 41, 588 (1970).
[4]Fermi motion of nucleons in beryllium will increase the effective energy and broaden the p_T^2 distribution. Our detection efficiency changes very slowly with p_T^2, and we have imposed no p_T^2 cut on our data, so the broadening causes no losses. On the other hand, Fermi motion was ignored when correcting for $t_{\min}$ effects. Thus we err on the conservative side in obtaining an upper limit.
[5]While completing this experiment, we received a paper from J. F. Martin *et al.* (to be published) in which they obtain an upper limit of 29 nb for ψ photoproduction at 18.2 GeV.
[6]Following the usual philosophy, we ignore any variation in $\gamma_\psi^2/4\pi$ between $m = 3.1$ GeV (appropriate to the storage-ring result) and $m = 0$ (appropriate to the photoproduction experiment). We also assume that ψN elastic scattering does not change appreciably when the incident ψ has zero mass. These conventional assumptions, though reasonable for ρ^0, ω, and φ, are not so clearly reasonable for a vector meson as massive as ψ.
[7]Since the ψ-N total cross section is lower than the φ-N total cross section, its elastic-scattering cross section is almost assuredly no steeper. From the $t_{\min}$ value, -0.39 GeV^2, one can easily calculate upper limits for any assumed t dependence.
[8]Because of the proximity of our measurement to threshold, the effective ψ-N energy at which these cross sections are measured is low. The final-state ψ momentum in the ψ-N center of mass is 1 GeV/c.

Measurement of $e^+e^- \to e^+e^-$ and $e^+e^- \to \mu^+\mu^-$†

J.-E. Augustin,* A. M. Boyarski, M. Breidenbach, F. Bulos, J. T. Dakin, G. J. Feldman, G. E. Fischer, D. Fryberger, G. Hanson, B. Jean-Marie,* R. R. Larsen, V. Lüth, H. L. Lynch, D. Lyon, C. C. Morehouse, J. M. Paterson, M. L. Perl, B. Richter, R. F. Schwitters, and F. Vannucci
Stanford Linear Accelerator Center, Stanford University, Stanford, California 94305

and

G. S. Abrams, D. Briggs, W. Chinowsky, C. E. Friedberg, G. Goldhaber, R. J. Hollebeek, J. A. Kadyk, G. H. Trilling, J. S. Whitaker, and J. E. Zipse
Lawrence Berkeley Laboratory and Department of Physics, University of California, Berkeley, California 94720
(Received 11 November 1974)

The reactions $e^+e^- \to e^+e^-$ and $e^+e^- \to \mu^+\mu^-$ have been measured at center-of-mass energies 3.0, 3.8, and 4.8 GeV and production angles of $50° < \theta < 130°$ over all azimuthal angles. Agreement with quantum electrodynamics is excellent. New limits for cutoff parameters in quantum-electrodynamic-breakdown models are given.

We report results from an experiment performed at the Stanford Linear Accelerator Center positron-electron storage ring (SPEAR I) to test with high precision the validity of quantum electrodynamics (QED) at large momentum transfers for the reactions

$$e^+e^- \to e^+e^-, \quad (1)$$

$$e^+e^- \to \mu^+\mu^-. \quad (2)$$

Data were collected at center-of-mass energies ($E_{\text{c.m.}}$) of 3.0, 3.8, and 4.8 GeV. A solenoidal magnetic spectrometer was used to measure angles, momenta, and charges of the final-state particles, resulting in a particularly stringent test of QED. While QED field theory has successfully explained results of previous experiments[1] on these reactions, ultimately deviations from QED are expected to occur at sufficiently large momentum transfers. Such deviations could be caused by photon-propagator modifications resulting from the recently observed large cross section for the reaction $e^+e^- \to$ hadrons,[2] or from the exchange of a neutral heavy boson like that required in the unified theories of weak and electromagnetic interactions, or from an intrinsic breakdown of QED itself.

SPEAR has two e^+e^- collision regions, each having an overlap size (σ_x, σ_y, σ_z) of approximately (1.5, 0.09, $20E_{\text{c.m.}}$) mm. The apparatus for this experiment, shown in Fig. 1, was positioned centrally about one of the interaction regions (IR), and subtended $0.65 \times 4\pi$ sr. The 3-m-diam×3-m-

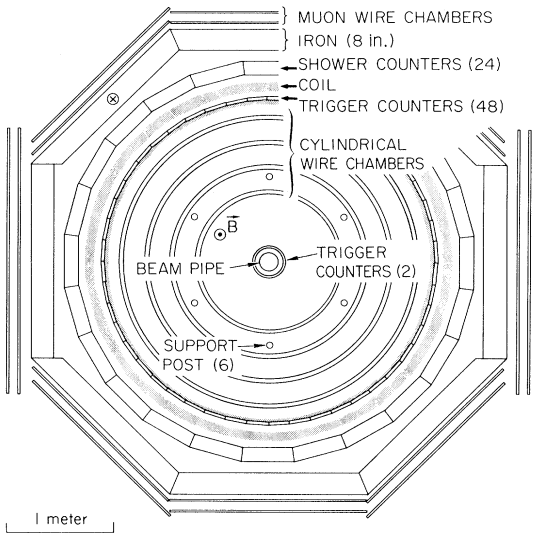

FIG. 1. End view of the solenoidal magnetic detector.

long coil produced a nominal 4-kG field coaxial with the beam direction (z axis). Particles entering the detector from the IR pass through a 0.15-mm stainless-steel vacuum chamber; an inner trigger counter (3-mm scintillator) for reducing cosmic-ray background; four sets of concentric cylindrical wire spark chambers, each set having one gap with wires at $\pm 2°$ and another at $\pm 4°$ with respect to the z axis; an outer trigger counter having 48 2.5-cm-thick plastic scintillation counters, which provide time-of-flight (TOF) information with a resolution of ± 0.5 nsec; the aluminum coil of 9 cm thickness; a cylindrical array of 24 lead-scintillator shower counters (5 radiation lengths) for electron identification; the 20-cm-thick iron return yoke of the magnet which also serves as a hadron filter; and finally two gaps of wire spark chambers which aid in muon-hadron separation. Iron endcaps provide a completely enclosed magnetic field, uniform to 3% over the active solid angle. The full azimuth is used while the acceptance in polar angle θ was 50° to 130°, limited by the outer trigger counters. A hardware trigger selected events having two or more charged particles by requiring occurrence of signals from the inner trigger counter and at least two outer-trigger-counter–shower-counter combinations during the beam crossing time.

The analysis programs constructed helical tracks from the cylindrical-chamber information, and determined the corresponding TOF and shower pulse height for each track. Events from Reactions (1) and (2) were separated from cosmic particles, background, and hadronic events by requiring that there be only two tracks which originated from an IR fiducial volume of 4-cm radius by 80-cm length,[3] were oppositely charged, had equal TOF within ± 3 nsec, were collinear to $\leq 10°$, and had momenta $p \geq E_{\mathrm{c.m.}}/4$. The latter two cuts eliminated e^+e^- or $\mu^+\mu^-$ events that radiated strongly and suppressed the processes $e^+e^- \to e^+e^-e^+e^-$ and $e^+e^- \to e^+e^-\mu^+\mu^-$. Separation of Reactions (1) and (2) was accomplished by using shower-counter pulse-height data, as shown in Fig. 2. A single cut at 70 clearly separates the e^+e^- from the $\mu^+\mu^-$ final states. Although hadron pairs (for example $\pi^+\pi^-$) could appear in the $\mu^+\mu^-$ class, a study of the muon-chamber information indicates no significant contamination

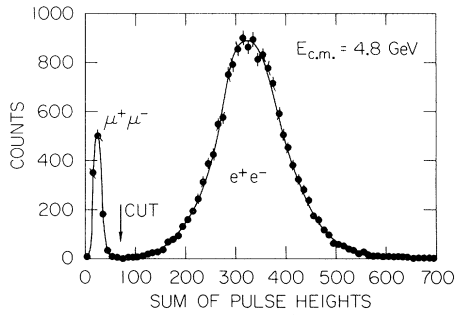

FIG. 2. Distribution of the sum of the shower-counter pulse heights for collinear events.

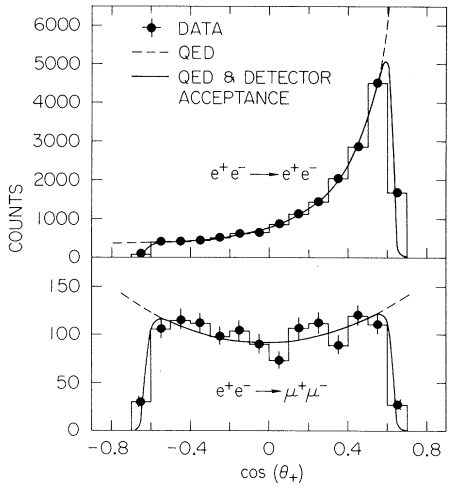

FIG. 3. Angular distribution of positive prongs for $e^+e^- \to e^+e^-$ and $e^+e^- \to \mu^+\mu^-$ at $E_{\mathrm{c.m.}} = 4.8$ GeV. The histograms give the observed counts, while the curves are QED normalized to total e^+e^- counts within $|\cos\theta_+| \leq 0.6$.

from this source.

The only significant hardware correction came from the shower-counter trigger, which was 94% to 98% efficient (depending on θ) for the $\mu^{\pm}$ signals ($\approx 100\%$ for $e^{\pm}$). No background subtraction was required, since we saw no QED candidates in noncolliding beam runs, comprising about 10% of the running time.

Using QED cross sections with radiative terms according to Berends, Gaemers, and Gastmans,[4] we normalized to the total e^+e^- counts within the interval $|\cos\theta_+|<0.6$, and made comparisons between corrected counts and theory for the shape of the e^+e^- angular distribution, for the $\mu^+\mu^-$ distribution, and for the $\mu^+\mu^-$-to-e^+e^- ratio. Agreement was good at all energies. Figure 3 shows one angular distribution. Total corrected counts over $|\cos\theta_+|<0.6$, and the ratio of observed to expected $\mu^+\mu^-$ events were as follows:

$E_{c.m.}$ (GeV)	e^+e^- counts	$\mu^+\mu^-$ counts	$\left(\frac{\text{expt.}}{\text{QED}}\right)_{\mu^+\mu^-}$
3.0	7671	563	0.95 ± 0.04
3.8	13419	1097	1.05 ± 0.03
4.8	15788	1241	1.01 ± 0.03

To establish limits on QED validity, we determine the limiting values that the parameter Λ can have in a modified photon-propagator model.[5] This is equivalent to modifying the QED amplitudes with form factors which we parametrize as

$$F(Q^2) = (1 \mp Q^2/\Lambda_{\pm}^2)^{-1} \approx 1 \pm Q^2/\Lambda_{\pm}^2, \quad (3)$$

where Q^2 is the photon four-momentum transfer and the +/− sign is used for establishing limits in Λ for positive or negative metrics. Our e^+e^- angular span is sufficiently large that separate limits can be extracted for spacelike (Λ_S) and timelike (Λ_T) photons, although different Λ_S and Λ_T would violate crossing symmetry as well as QED. The modified cross section for $e^+e^- \to e^+e^-$ is

$$\frac{d\sigma}{d\Omega} = \frac{\alpha^2}{2s}\left(\frac{q'^4+s^2}{q^4}|F_S|^2 + \frac{2q'^4}{q^2 s}\mathrm{Re}(F_S F_T^*) + \frac{q'^4+q^4}{s^2}|F_T|^2\right), \quad (4)$$

where $q^2 = -s\sin^2\theta/2$; $q'^2 = -s\cos^2\theta/2$; $s = E_{c.m.}^2$; $F_S = 1 \pm q^2/\Lambda_{S\pm}^2$; and $F_T = 1 \pm s/\Lambda_{T\pm}^2$. For $e^+e^- \to \mu^+\mu^-$

$$\frac{d\sigma}{d\Omega} = \frac{\alpha^2}{4s}[1 + \cos^2\theta + (1-\beta_\mu^2)\sin^2\theta]|F_T|^2. \quad (5)$$

By simultaneously fitting both the $\mu^+\mu^-$ and e^+e^- data with the same Λ_T parameter (i.e., assuming μ-e universality) a much more sensitive test of QED can be made than is possible for the e^+e^- data alone.

As an alternate QED modification method, one can insert form factors at the $ee\gamma$ and $\mu\mu\gamma$ vertices. This formulation is more suitable for establishing limits on the point structure of electrons and muons, as well as on μ-e universality. In a similar way, we parametrize the electron and muon form factors by $F_{e,\mu}(Q^2) = 1 \pm Q^2/\Lambda_{e,\mu}^2$.

The various cutoff constants $1/\Lambda^2$ were found by fitting the $\mu^+\mu^-$ and/or e^+e^- angular distributions by the modified QED cross sections normalized to the total e^+e^- counts within $|\cos\theta| \le 0.6$ (the normalization is a function of Λ also). Table I gives the results of the fits, with the corresponding lower limits for $\Lambda_{\pm}$ (95% confidence level) for the various breakdown models. This is the first time that separate spacelike and timelike limits have been established for process (1). The assumption of a single form factor for both

TABLE I. Weighted averages over the three energies of the fitting parameters and 95% cutoff limits established from the e^+e^- data, and from the $\mu^+\mu^-$ data together with e^+e^-, for QED breakdown models with (a) separate form factors for spacelike and timelike photons, (b) same form factors for spacelike or timelike photons, and (c) separate form factors at the $ee\gamma$ and $\mu\mu\gamma$ vertices.

Data Used	Model	Fitted Parameters (Λ in GeV)	Λ at 95% C.L. (GeV) pos. metric	neg. metric
ee only	a	$1/\Lambda_S^2 = 0.0008 \pm 0.0022$ $1/\Lambda_T^2 = 0.0013 \pm 0.0031$ correl. coeff. = 0.82	$\Lambda_{S+} > 15$ $\Lambda_{T+} > 13$	$\Lambda_{S-} > 19$ $\Lambda_{T-} > 16$
	b	$1/\Lambda^2 = 0.0007 \pm 0.0022$	$\Lambda_+ > 15$	$\Lambda_- > 19$
$\mu\mu$ and ee	a	$1/\Lambda_S^2 = 0.0003 \pm 0.0013$ $1/\Lambda_T^2 = 0.0001 \pm 0.0005$ correl. coeff. = 0.23	$\Lambda_{S+} > 21$ $\Lambda_{T+} > 33$	$\Lambda_{S-} > 23$ $\Lambda_{T-} > 36$
	b	$1/\Lambda^2 = 0.0002 \pm 0.0004$	$\Lambda_+ > 35$	$\Lambda_- > 47$
	c	$1/\Lambda_e^2 = 0.0004 \pm 0.0011$ $1/\Lambda_\mu^2 = 0.0014 \pm 0.0021$ correl. coeff. = −0.97	$\Lambda_{e+} > 21$ $\Lambda_{\mu+} > 27$	$\Lambda_{e-} > 19$ $\Lambda_{\mu-} > 16$

spacelike and timelike photons gives cutoffs $\Lambda_+ > 35$ GeV and $\Lambda_- > 47$ GeV, which are considerably larger than the previous highest limits ($\Lambda_+ > 14.5$ GeV, $\Lambda_- > 23.6$ GeV) set by Beron *et al.*[1] No deviation of either the electron or muon form factor from unity has been observed, the cutoff parameters being always larger than 16 GeV. Our limit $\Lambda_{\mu e}$ on μ-e universality, defined by $1/\Lambda_{\mu e}^2 \equiv 1/\Lambda_\mu^2 - 1/\Lambda_e^2$, is $\Lambda_{\mu e^+} > 13$ GeV and $\Lambda_{\mu e^-} > 15$ GeV determined from the (correlated) difference between $1/\Lambda_\mu^2$ and $1/\Lambda_e^2$ from Table I.

We wish to acknowledge the many people who contributed to the construction of SPEAR and the magnetic detector, and the operators for running the storage ring. Their efforts were essential to the success of this experiment.

†Work supported by the U. S. Atomic Energy Commission.

*Laboratoire de l'Accélérateur Linéaire, Centre d'Orsay de l'Université de Paris, 91 Orsay, France

[1]B. L. Beron *et al.*, Phys Rev. Lett. 33, 663 (1974); H. Newman *et al.*, Phys. Rev. Lett. 32, 483 (1974); M. Bernardini, Phys. Lett. 45B, 510 (1973); B. Borgia *et al.*, Lett. Nuovo Cimento 3, 115 (1972); V. Alles-Borelli *et al.*, Nuovo Cimento 7A, 330 (1972).

[2]G. Tarnopolsky *et al.*, Phys. Rev. Lett. 32, 432 (1974); J.-E. Augustin *et al.*, to be published.

[3]The detector resolution was such that the closest distance of approach to the IR origin for collinear tracks could be determined to ±7 mm in the radial position and ±1 cm in the z direction.

[4]F. A. Berends, K. J. F. Gaemers, and R. Gastmans, Nucl. Phys. B68, 541 (1974) and B63, 381 (1973). We are indebted to these authors for supplying to us their computer program. Radiative corrections were -0.14 (-0.07), -0.13 (-0.06), and -0.12 (-0.03) for e^+e^- $(\mu^+\mu^-)$ at $\cos\theta_+ = -0.5$, 0, and 0.5, respectively.

[5]S. D. Drell, Ann. Phys. (New York) 4, 75 (1958); T. D. Lee and G. C. Wick, Nucl. Phys. B9, 209 (1969).

SU(4) Symmetry and the Possible Existence of New Hadrons*

S. Okubo, V. S. Mathur, and S. Borchardt
University of Rochester, Rochester, New York 14627
(Received 25 November 1974)

We derive SU(4) mass formulas taking mixing, whenever it arises, fully into account. With the masses of the usual hadrons and that of the newly discovered resonance ψ as input, we predict the masses of the new 1^- and 0^- mesons as well as the $\frac{1}{2}^+$ and $\frac{3}{2}^+$ baryons.

Recently a new resonance (hereafter called ψ) has been reported[1] in $e\bar{e} \to$ hadrons and $p + \mathrm{Be} \to e\bar{e} + \ldots$ at a mass value of 3.105 ± 0.003 GeV and a very narrow width $\Gamma < 1.3$ MeV. Assuming that it is a vector particle, we have recently proposed[2] the possibility that this resonance belongs to a $15 \oplus 1$ dimensional representation of the SU(4) group. This hypothesis is presently consistent with the various experimental features such as the total production cross section and the width that have been reported.

If our suggestion is correct, it opens up a whole world of new particles carrying a new quantum number, usually referred to as charm. In this note, we discuss the classification of these new particles under SU(4), and derive the SU(4) mass formulas for 1^- and 0^- mesons as well as for $\frac{1}{2}^+$ and $\frac{3}{2}^+$ baryons. With the mass of the ψ as input, we obtain numerical predictions for the masses of the new mesons and baryons. We assume that SU(4) symmetry is broken by the interaction[3]

$$H' = T_8 + \alpha T_{15}, \tag{1}$$

where T_8 and T_{15} belong to the same 15-dimensional representation of SU(4).

As suggested we assume that the 1^- mesons belong to a $15 \oplus 1$ dimensional representation of SU(4), which we may denote by V^α ($\alpha = 0, 1, \ldots 15$). Note that if we consider as usual that mesons are quark-antiquark structures, this is the SU(4) representation we obtain from $4 \otimes \bar{4} = 15 \oplus 1$. The SU(3) decomposition of the 15-plet is

$$15 \supset 8 \oplus 3 \oplus \bar{3} \oplus 1. \tag{2}$$

The components $V^{1,\ldots 8}$ and V^{15}, belonging to the $8 \oplus 1$ representation, describe the nonet of vector mesons. The representation 3 contains an SU(2) doublet $C_u(V), C_d(V)$ and an SU(2) singlet $C_s(V)$ with the quantum numbers displayed in Table I. The SU(3) representation $\bar{3}$ contains the corre-